FUNCTION FIELD METHODOLOGY FOR ESTIMATING SPECTRAL MARINE REFLECTANCE FROM ADEOS-II GLOBAL IMAGER DATA

Robert FROUIN [1] and Bruno PELLETIER [2]

[1] Scripps Institution of Oceanography
University of California, San Diego
9500 Gilman Drive, La Jolla, CA 92093-0224, USA
rfrouin@ucsd.edu

[2] Institut de Mathématiques et de Modélisation de Montpellier
Université Montpellier II, CC 051
Place Eugène Bataillon, 34095 Montpellier Cedex 5, France
pelletier@math.univ-montp2.fr

Abstract

A general function field methodology for estimating ocean color variables from space is applied to the retrieval of spectral marine reflectance from Global Imager (GLI) data. The top-of-atmosphere GLI reflectance vectors, after correction for molecular effects, are considered as explanatory variables conditioned by the angular geometry. The inverse problem, therefore, is viewed as a collection of similar inverse problems, continuously indexed by the angular variables. The solution is in the form of a field of nonlinear regression models over the set of permitted values for the angular variables. The selected models, for reasons of approximation theory, are fields of shifted ridge functions. The fields constructed on synthetic GLI data for Case 1 waters are robust to noise, they handle well situations of weakly and strongly absorbing aerosols, and the retrievals are accurate in both oligotrophic and productive waters. In the presence of 1% noise, the RMS error is 0.0006 (4.2%) at 412 nm and 0.0001 (1.5%) at 545 nm, i.e., well within the acceptable limits for quantitative biology applications. The theoretical results, and the possible extensions, show the potential of the function field methodology for operational estimation of marine reflectance from GLI data.

Keywords: ocean color, marine reflectance, remote sensing, function fields, statistical inverse problems

1 Introduction

Ocean color observations from space are affected by a variety of interfering processes associated with propagation of electromagnetic radiation in the atmosphere-surface system. In clear sky conditions, these processes are gaseous absorption, molecular scattering, aerosol scattering and absorption, and surface reflection. In cloudy conditions, scattering by cloud droplets makes it very difficult to sense the surface, except when clouds are optically thin. The influence of the atmosphere and surface must be removed in the satellite imagery to give access to water-leaving radiance, or equivalently diffuse marine reflectance, the signal that contains information about the water body. This is referred to as atmospheric correction, even though surface effects are also removed. Gaseous absorption is generally easy to handle since ocean color sensors observe in atmospheric windows, and molecular scattering can be computed accurately. The influence of scattering by aerosols, highly variable in space and time, and of reflection by a wind-ruffled surface, which may exhibit whitecaps, is more difficult to correct. In coastal regions, high spatial variability and proximity of land introduce further difficulty. Fundamentally, accurate atmospheric correction is not easy to achieve since the contribution of the water body may only represent a small fraction of the measured signal, typically 10% in the blue over clear waters and a few percent over turbid waters.

The standard approach for atmospheric correction, first suggested by Gordon [1], consists of (1) estimating the aerosol reflectance in the red and near infrared spectral region where the ocean can be considered totally absorbing (i.e., black), and (2) extrapolating the aerosol reflectance to the shorter ocean color wavelengths. Algorithms based on this approach have been developed successfully and employed for the operational processing of data from most satellite ocean color sensors [2, 3, 4, 5, 6, 7, 8]. In the coastal zone where waters often contain inorganic material, the assumption of null water reflectance in the red and near infrared is not valid, and improvements to the standard algorithms have been proposed [9, 10, 11, 12, 13]. For Global Imager (GLI) onboard the Advanced Earth Observation Satellite II (ADEOS-II), the atmospheric correction scheme includes an iterative procedure for evaluating water reflectance in the near infrared that accounts for chlorophyll, suspended sediment, and dissolved organic matter [8]. The scheme also detects the presence of absorbing aerosols by exploiting observations in the ultraviolet, yielding more accurate retrievals of marine reflectance in the blue in the presence of such aerosols.

An alternative approach to atmospheric correction is to perform a direct mapping of the measured top-of-atmosphere (TOA) reflectance to the marine reflectance, where the direct mapping solution to the statistical inverse problem is defined as a regression function. In defining a suitable regression estimate, several considerations have to be taken into account. First, the TOA reflectance depends on angular variables, namely sun zenith angle, view zenith angle, and relative azimuth angle. The spectral components of the TOA reflectance vector are therefore naturally correlated via geometry, possibly in a complex manner, and correlation between explanatory variables is known to reduce the efficiency of statistical modeling techniques. Second, angular variables affect essentially the atmosphere and surface contributions to the TOA reflectance. They do not provide information on marine reflectance, which is fairly isotropic. Yet, the angular variables need to be accounted for in the inversion procedure since they introduce some variability in the measured signal. This leads to the problem where vectors of TOA reflectance are treated as explanatory variables conditioned by the less informative angular variables, and where the inverse problem is viewed as a collection of similar inverse problems, continuously indexed by the angular variables. The proposed solution consists in attaching an inverse model to each value of the angular variables, with the attachment varying smoothly with the angular variables. Such a solution is mathematically formalized as a function field over the set of permitted values for the angular variables.

The function field methodology for inverting satellite data influenced by conditioning variables was introduced generally by Pelletier and Frouin [14], then developed for the remote sensing of chlorophyll concentration [15]. It was recently extended to the retrieval of diffuse marine reflectance [16]. Shifted ridge functions were selected in the modeling because of their good approximation properties [17]. The statistical models were evaluated on synthetic data and tested on Sea-viewing Wide Field-of-view Sensor (SeaWiFS) imagery, taking into account noise in the data. Theoretical performance was adequate in terms of accuracy, robustness, and generalization capabilities, suggesting that the methodology might provide more accurate retrievals of marine reflectance than standard algorithms in the presence of absorbing aerosols and in productive waters. The satellite estimates obtained with the ridge function fields were also more realistic than those using standard atmospheric correction. The studies further showed that large levels of noise, due to uncertainties in radiation transfer modeling and radiometry, could be managed if the noise distribution were known or estimated.

In the following, the potential of the function field methodology for atmospheric correction of GLI ocean-color imagery is evaluated. The objective is to demonstrate that accurate mapping can be obtained between GLI spectral observations and spectral marine reflectance for a realistic model of Case 1 waters. The procedure to retrieve marine reflectance by use of ridge function fields is described. Performance is quantified using synthetic data, and errors are analyzed as a function of angular geometry, geophysical conditions, and noise distribution. Practical ways of estimating the noise distribution are suggested. Extension of the methodology to optically complex (Case 2) waters is discussed, as well as other applications.

2 Inversion by Use of Ridge Function Fields

Given a prior distribution on the input parameters to a radiative transfer model and a noise distribution, the solution to the statistical inverse problem considered in [14, 15, 16] is defined as the regression function of the marine reflectance to the TOA reflectance and angular variables. Formally, let $\mathbf{X}$ and $\mathbf{Y}$ be the (spectral) vectors of TOA reflectance and marine reflectance, taking values in $\mathbb{R}^d$ and $\mathbb{R}^{d'}$, respectively. Let $\mathbf{T}$ be the vector of cosines of the angular variables valued in some compact subset $\mathcal{T} \subset \mathbb{R}^3$. Then the regression function m of $\mathbf{Y}$ on $\mathbf{X}$ and $\mathbf{T}$ is given by $m(\mathbf{x}, \mathbf{t}) = \mathbb{E}_{\mathbf{X}=\mathbf{x},\mathbf{T}=\mathbf{t}}[\mathbf{Y}|\mathbf{X}, \mathbf{T}]$ and performs a direct mapping to the vector of marine reflectance values. Owing to the complexity of radiative transfer models, though, m may not be expressed analytically. Therefore m must be approximated numerically. To this aim, the approach developed in [14, 15, 16] consists in i) sampling the forward operator (i.e., the radiative transfer model) according to the prior distribution, ii) defining a reasonable noise distribution, and iii) estimating m from the simulated data $(\mathbf{X}_i, \mathbf{T}_i, \mathbf{Y}_i)$, $i = 1, \ldots, n$. Function fields over $\mathcal{T}$ are introduced as models for m which reflect the different roles played by the TOA reflectance and the angular variables.

The function fields considered for the estimation of the diffuse marine reflectance are fields of shifted ridge functions, called ridge function fields in short. A ridge function on $\mathbb{R}^d$ is a function of the form $h(\mathbf{a}.\mathbf{x})$, where h is some map on $\mathbb{R}$ and $\mathbf{a}.\mathbf{x}$ is the standard inner product of $\mathbf{a}$ and $\mathbf{x}$ on $\mathbb{R}^d$. Approximation by ridge function refers to approximation by linear combinations of some number K of

ridge functions, or their shifted versions, written as follows:

$$f(\mathbf{x}) = \sum_{i=1}^{K} c_i h(\mathbf{a}_i.\mathbf{x} + b_i). \tag{2.1}$$

Ridge function fields over $\mathcal{T}$ are constructed by replacing the parameters $\mathbf{a}_i$, b_i, and c_i in (2.1) with functions of $\mathbf{t}$, lying in some finite-dimensional subspace of functions. Ridge function fields are known to span a dense set when the number of parameters tend to infinity [17], and it may be shown that, under mild conditions, ridge function fields adjusted by least-squares are strongly universally consistent nonparametric regression estimates. Thus the procedure is convergent as for estimating m.

More specifically, let $\mathbf{x} \in \mathbb{R}^d$ and $\mathbf{y} \in \mathbb{R}^{d'}$ be the values taken by the (spectral) vectors of the TOA reflectance and marine reflectance, respectively. Let $\mathbf{t} = (\cos\theta_s, \cos\theta_v, \cos\Delta\varphi)^t$ be the value taken by the vector of cosines of the angular variables, taking values in the set $T = [\frac{1}{2}; 1] \times [\frac{1}{2}; 1] \times [-1; 1]$. Let

$$E(\mathbf{a}_1, ..., \mathbf{a}_n, b_1, ..., b_n) = \text{span}\,\{h(\mathbf{a}_1.\mathbf{x} + b_1), ..., h(\mathbf{a}_n.\mathbf{x} + b_n)\}, \tag{2.2}$$

where $h : \mathbb{R} \to \mathbb{R}$, i.e., $E(\mathbf{a}_1, ..., \mathbf{a}_n, b_1, ..., b_n)$ is the vector space spanned by the linear combinations of the $h(\mathbf{a}_i.\mathbf{x} + b_i)$. For the retrieval of $\mathbf{y}$ from $\mathbf{x}$, we consider function fields $\zeta : \mathcal{T} \to E^{d'}(\mathbf{a}_1, ..., \mathbf{a}_n, b_1, ..., b_n)$ such that

$$\zeta(\mathbf{t})^j(\mathbf{x}) = \sum_{i=1}^{n} c_i^j(\mathbf{t}) h(\mathbf{a}_i.\mathbf{x} + b_i), \tag{2.3}$$

for $j = 1, ..., d'$, and the statistical model relative to the j^{th} component of $\mathbf{y}$ is written as

$$y^j = \zeta(\mathbf{t})^j(\mathbf{x}) + \epsilon^j. \tag{2.4}$$

where ϵ^j represents the residual of the modeling. The functions c_i^j are defined by multi-linear interpolation on a $2 \times 2 \times 3$ regular grid covering T, i.e., they are piecewise-differentiable functions, each of whose depends on 12 scalars, but smoother models mau easily be implemented. These scalars, together with the $\mathbf{a}_i$'s and the b_i's constitute the free parameters of the model. The model is adjusted by minimizing the sum of the squared errors $\mathcal{E}$ on the data defined by

$$\mathcal{E} = \frac{1}{n} \sum_{i=1}^{n} \|\zeta(\mathbf{t}_i)(\mathbf{x}_i) - \mathbf{y}_i\|^2, \tag{2.5}$$

where $\|.\|$ is the usual Euclidean norm on $\mathbb{R}^{d'}$. In practice, the components of $\mathbf{y}$ are normalized linearly between -1 and 1, and the minimization of $\mathcal{E}$ is carried out using a stochastic gradient descent procedure (see Pelletier and Frouin [15] for details).

3 Model Construction and Performance

To determine the inverse (regression) model parameters, we generated a statistically significant data set of about 62,000 joint samples of TOA and marine reflectance using a coupled ocean-surface-atmosphere radiative transfer code [18]. This code takes into account the essential physics of the problem, i.e., gaseous absorption, scattering by molecules and aerosols, absorption by aerosols, Fresnel reflection at the interface, and backscattering by the water body. The TOA reflectance was simulated in the GLI spectral bands centered at 380, 412, 443, 460, 520, 545, 666, 749, and 865 nm and was corrected for molecular effects. The marine reflectance was simulated according to Morel and Maritorena [19], valid for Case 1 waters. The data set encompassed the major sources of variability (geometric, geophysical) and included three aerosols models (marine, continental, and urban) in varied mixtures. It was randomly split into two subsets $\mathcal{D}_e^0$ and $\mathcal{D}_v^0$, used respectively for adjusting and validating the statistical inverse models. For robustness assessments, we also generated noisy versions of the previous subsets, hereafter denoted by $\mathcal{D}_e^\nu$ and $\mathcal{D}_v^\nu$, of $\mathcal{D}_e^0$ and $\mathcal{D}_v^0$, by adding some amount of noise to the TOA reflectance. The selected noise is the sum of correlated and uncorrelated components, and is defined by:

$$\tilde{\mathbf{x}} = \mathbf{x} + \nu^c \mathbf{x} + \left(\nu_1^{uc} x^1, ..., \nu_8^{uc} x^8\right)^t, \tag{3.1}$$

where $\tilde{\mathbf{x}}$ is a noisy version of TOA reflectance vector $\mathbf{x}$, and $\nu^c, \nu_1^{nc}, ..., \nu_8^{nc}$ are random variables uniformly distributed on the interval $[-\frac{\nu}{200}; \frac{\nu}{200}]$, with the total amount of noise ν in percent.

For the models we selected empirically (i.e., via simulations) the sufficient number of $K = 15$ basis functions, and constructed two fields ζ^0 and ζ^1 with $K = 15$. The first one, ζ^0, was adjusted on $\mathcal{D}^0$. In the case of ζ^1, we added a noise amount of 1% to the TOA reflectance during the execution of the minimization procedure, where the added noise satisfies (3.1). Note that this is not equivalent to adjusting the fields on $\mathcal{D}_e^1$. As indicated in the previous section, the parameter maps were defined by multilinear interpolation on a $2 \times 2 \times 3$ regular grid covering $\mathcal{T}$, and

the fields were optimized via a dedicated stochastic gradient descent algorithm.

The theoretical performance of the models is summarized in Table 1, which gives, on a component-per-component basis, the Root Mean Squared error (RMS) and the Relative Root Mean Squared error (RMSR) of ζ^ν evaluated on $\mathcal{D}_e^{\nu'}$, for all combinations of $\nu, \nu' = 0, 1$. Biases are not indicated in the table, since the estimation is practically unbiased for all fields. These statistical measures show that the fields present good validation properties, even in the presence of noise. As expected, for a noise level of $\nu\%$ on the TOA reflectance, the best retrievals are achieved by ζ^ν. At 380 nm, for example, the relative error is doubled from 2.8 to 5.6% when ζ^0 is applied to the noisy data, but is reduced to 4.2% when using ζ^1. This illustrates the importance of the noise distribution, defined prior to the construction of the models. The marine reflectance estimations are accurate over the whole range of values, as depicted by Figs. 1 and 2, which display plots of estimated versus expected reflectance. The distribution of the residuals (i.e., estimation errors) depends on the aerosol optical thickness (τ_a). The conditional quantiles of orders 5, 25, 75, and 95% spread with increasing τ_a (Fig. 3). However, the errors are weakly dependent on the aerosol type and no trends are revealed (not shown here). Absorbing aerosols, in particular, are handled adequately by the function field methodology, which, unlike standard algorithms, processes information in spectral bands sensitive to aerosol absorption (i.e., in the ultraviolet and blue). The scattering angle also influences the results, evidenced by a slight error increase at low and high scattering angles (Fig. 4). This is expected since the aerosol phase function (i.e., the atmospheric interference) generally exhibits smaller values at intermediate backscattering angles (120-140 degrees). The relation between reflectance ratio (443 and 545 nm) and chlorophyll-a concentration obtained using estimated reflectance is slightly degraded; see Fig. 5 for reflectance estimated by ζ^0 from 1% noisy data. In this case, the reflectance ratio is estimated with a RMS accuracy of about 0.3 (Fig. 6), which translates into a relative RMS error of about 10% on the chlorophyll-a concentration.

4 Conclusion

The statistical methodology presented above allows one to estimate directly spectral marine reflectance from space in the context of regression analysis, by considering the TOA measurements as explanatory variables conditioned by the geometry of the observation process. This leads to a framework where the solution

is expressed as a function field. The inversion scheme is robust, with good generalization capability, and computationally efficient.

The results obtained with GLI synthetic data over Case 1 waters suggest that the methodology has the potential for improving the accuracy of the inversion compared with the current GLI atmospheric correction algorithm, as it can handle noise and different types of aerosols, including absorbing ones, and provide a uniform error over the entire range of marine reflectance values. In the presence of 1% noise, marine reflectance at 380, 412, 443, 460, 520, and 545 nm is retrieved with a RMS error of 0.0006 (4.2%), 0.0006 (3.7%), 0.0004 (3.1%), 0.00031 (2.7%), 0.0001 (1.1%), and 0.0001 (1.5%), respectively. This error meets the requirements of 0.001-0.002 in the blue for quantitative biology applications, and it allows discrimination of at least 30 classes of chlorophyll-a concentration in the range 0.03-30 $\mathrm{mg\,m^{-3}}$. Let us emphasize, however, that the results are theoretical. To conclude about practical suitability, the methodology needs to be tested on actual GLI data, acquired in varied oceanic and atmospheric regimes.

The noise structure, or more precisely the noise distribution, is an essential factor for the robustness of an inversion algorithm, and its influence is well revealed through the simulations. Further investigations are required to get a precise idea of the statistical properties of the total discrepancies between radiative transfer simulations and GLI measurements, including instrument noise, calibration errors, and model uncertainties. As pointed out by Frouin and Pelletier [16], using concomitant satellite observations and in-situ measurements to investigate the noise statistical properties might not be feasible because of the lack or insufficient number of in-situ measurements, and a reasonable alternative would be to compare satellite measurements with elements of the range of the forward model.

The methodology is general, therefore it can be extended to other sets of models. In particular, one may attempt to extend the retrievals of marine reflectance to optically complex Case 2 waters, and to estimate directly, by designing specific fields of vector-valued maps, the variables affecting the marine reflectance, i.e., chlorophyll-a concentration, yellow substance absorption, and sediment concentration. Since these variables, which characterize water composition, are the variables of interest in bio-geochemistry applications, the direct approach would be more efficient that a two-step estimation via the marine reflectance. But in this case performance will be affected by the complexity of the relation between marine reflectance and water composition variables. These extensions of the func-

tion field methodology, as well as the application to actual GLI data and evaluation against in-situ measurements, give a perspective for future work.

Acknowledgments

Support for this work was provided by the Japan Aerospace Exploration Agency (under Contract No. 03/JAXA/AEO No. 1208001) and by the National Aeronautics and Space Administration (under Grant No. NN05GR20G). We thank Mr. John McPherson, Scripps Institution of Oceanography, La Jolla, California, for providing technical assistance.

References

[1] H. R. Gordon: Removal of atmospheric effects from satellite imagery of the oceans, *Appl. Opt.*, **17**, 1631-1636, 1978.

[2] M. Viollier, D. Tanr, and P.-Y. Deschamps: An algorithm for remote sensing of water color from space, *Boundary-Layer Meteor.*, **18**, 247-267, 1980.

[3] H. R. Gordon and M. Wang, 1994: Retrieval of water-leaving radiance and aerosol optical thickness over the oceans with SeaWiFS: a preliminary algorithm, *Appl. Opt.*, **33**, 443-452, 1994.

[4] H. R. Gordon: Atmospheric correction of ocean color imagery in the Earth Observing System era, *J. Geophys. Res.*, **102**, 17107-17118, 1997.

[5] H. Fukushima, A. Higurashi, Y. Mitomi, T. Nakajima, T. Noguchi, T. Tanaka, and M. Toratani: Correction of atmospheric effects on ADEOS/OCTS ocean color data: Algorithm description and evaluation of its performance, *J. Oceanogr.*, *54*, 417-430, 1998.

[6] D. Antoine, and A. Morel: A multiple scattering algorithm for atmospheric correction of remotely sensed ocean colour (MERIS instrument): principle and implementation for atmospheres carrying various aerosols including absorbing ones, *Int. J. Remote Sens.*, **20**, 1875-1916, 1999.

[7] B.-C. Gao, M. J. Montes, Z. Ahmad, and C. O. Davis: Atmospheric correction algorithm for hyper-spectral remote sensing of ocean color from space, *Appl. Opt.*, **39**, 887-896, 2000.

[8] M. Toratani, H. Fukushima, H. Murakami, and A. Tanaka: Atmospheric correction scheme for GLI with absorptive aerosol correction, *J. Oceanogr.*, **63**, 525-532, 2007.

[9] P. E. Land and J. D. Haigh: Atmospheric correction over Case 2 waters using an iterative fitting algorithm, *Appl. Opt.*, **35**, 5443-5451, 1996.

[10] G. F. Moore, J. Aiken, and S. J. Lavender: The atmospheric correction of water colour and the quantitative retrieval of suspended particulate matter in Case 2 waters: Application to MERIS, *Int. J. Remote Sen.*, **20**, 1713-1733, 1999.

[11] K. G. Ruddick, F. Ovidio, and M. Rijkeboer, Atmospheric correction of SeaWiFS imagery for turbid and inland waters, *Appl. Opt.*, **39**, pp. 897-912, 2000.

[12] C. Hu, K. L. Carder, and F. Muller-Karger: Atmospheric correction of SeaWiFS imagery over turbid coastal waters: A practical method. *Remote Sens Environ.*, **74**, 195-206, 2000.

[13] S. J. Lavender, M. H. Pinkerton, G. F. Moore, J. Aiken, and D. Blondeau-Patissier: Modification of the atmospheric correction of SeaWiFS ocean colour images over turbid waters. *Cont. Shelf Res.*, **25**, 539-555, 2005.

[14] B. Pelletier and R. Frouin: Fields of nonlinear regression models for inversion of satellite data, *Geophys. Res. Lett.*, **31**, L16304, 2004.

[15] B. Pelletier and R. Frouin: Remote sensing of chlorophyll-a concentration by use of ridge function fields, *Appl. Opt.*, **20**, 1735-1746, 2006.

[16] R. Frouin and B. Pelletier: Fields of nonlinear regression models for atmospheric correction of satellite ocean color imagery, *Remote Sen. Environ.*, **111**, 450-465, 2007.

[17] B. Pelletier: Approximation by ridge function fields over compact sets, *J. Approx. Theory*, **129**, 230-239, 2004.

[18] E. Vermote, D. Tanre, J.-L. Deuze, M. Herman, and J.-J. Morcrette: Second simulation of the satellite signal in the solar spectrum: An overview, *IEEE Trans. Geosci. Remote Sen.*, **35**, 675-686, 1997.

[19] A. Morel and S. Maritorena: Bio-optical properties of oceanic waters: A reappraisal, *J. Geophys. Res.*, **106**, 7163-7180, 2002.

Table 1: Root Mean Squared error (RMS) and Root Mean Squared Relative error (RMSR) for the models ζ^0 and ζ^1, evaluated on the non-noisy construction and validation sets ($\mathcal{D}_e^0$ and $\mathcal{D}_v^0$), and on a 1%-noisy version of them ($\mathcal{D}_e^1$ and $\mathcal{D}_v^1$).

		FIELD ζ^0					
	λ (nm)	380	412	443	460	520	545
$\mathcal{D}_e^0$	RMS	0.000357	0.000362	0.000221	0.000165	$5.33e-05$	$6.64e-05$
	RMSR	0.027290	0.025008	0.019108	0.016000	$6.19e-03$	$7.69e-03$
$\mathcal{D}_v^0$	RMS	0.000357	0.000363	0.000221	0.000165	$5.36e-05$	$6.63e-05$
	RMSR	0.028168	0.025763	0.019607	0.016372	$6.23e-03$	$7.65e-03$
$\mathcal{D}_e^1$	RMS	0.000901	0.000846	0.00055	0.000422	0.000150	0.000187
	RMSR	0.055998	0.049971	0.04171	0.036165	0.016896	0.021906
$\mathcal{D}_v^1$	RMS	0.000888	0.000833	0.000543	0.000417	0.000152	0.000186
	RMSR	0.056408	0.049936	0.041885	0.036508	0.017140	0.021722
		FIELD ζ^1					
$\mathcal{D}_e^0$	RMS	0.000434	0.000431	0.000267	0.000202	$6.96e-05$	$8.48e-05$
	RMSR	0.028771	0.025905	0.021234	0.018443	$8.02e-03$	$9.91e-03$
$\mathcal{D}_v^0$	RMS	0.000433	0.000433	0.000267	0.000202	$7.18e-05$	$8.56e-05$
	RMSR	0.029120	0.026096	0.021457	0.018729	$8.30e-03$	$9.95e-03$
$\mathcal{D}_e^1$	RMS	0.000654	0.000631	0.000402	0.000309	$9.76e-05$	0.000132
	RMSR	0.041901	0.037426	0.031563	0.027655	$1.12e-02$	0.015271
$\mathcal{D}_v^1$	RMS	0.000646	0.000624	0.000397	0.000305	0.000100	0.000131
	RMSR	0.041971	0.037267	0.031546	0.027777	0.011457	0.015066

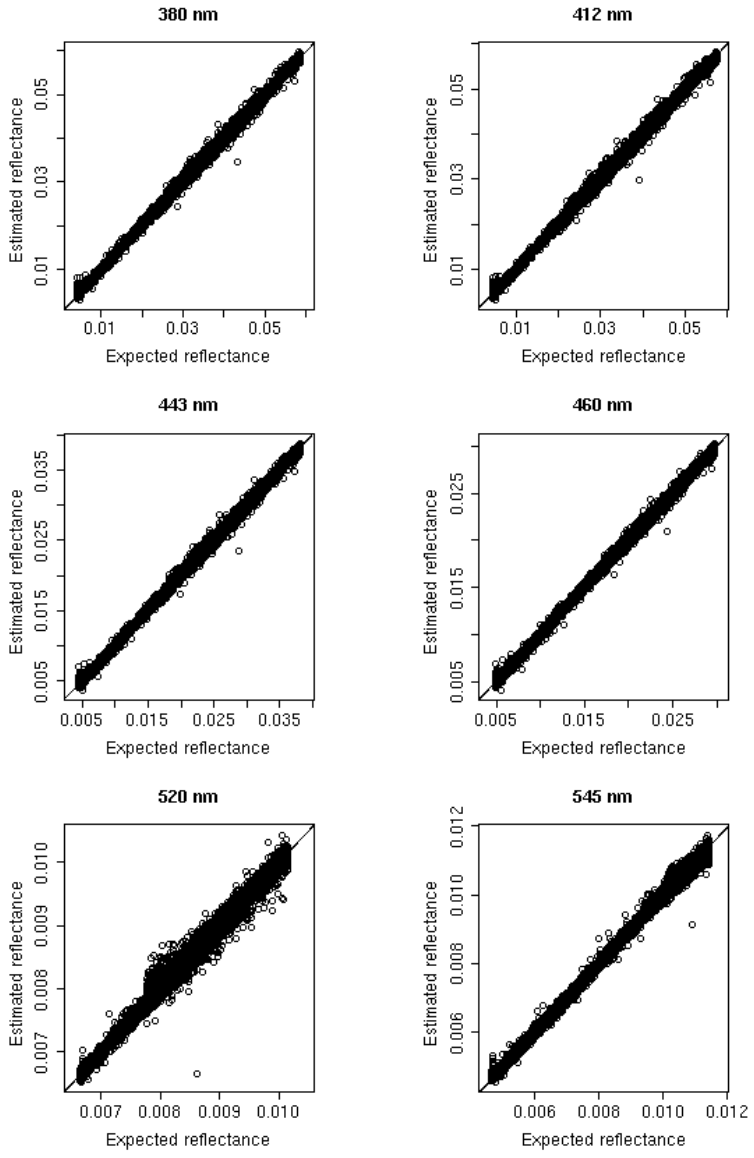

Figure 1: Estimated versus expected above-surface marine reflectance for model ζ^0 on non-noisy GLI data.

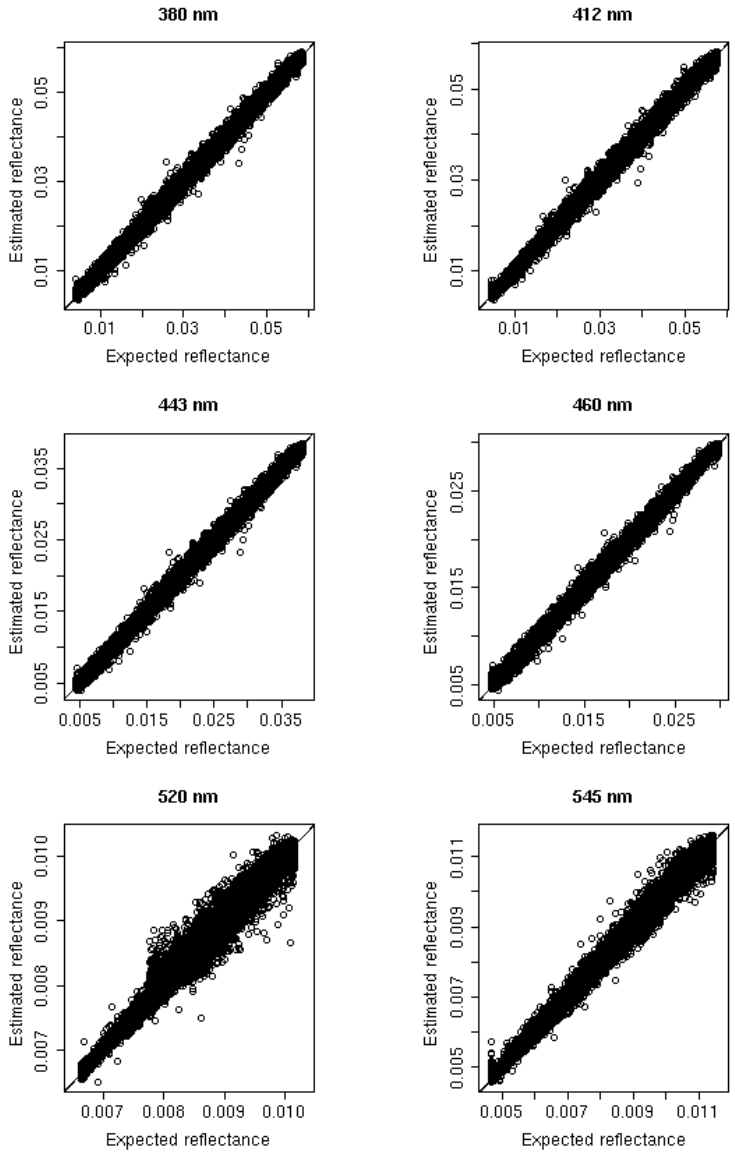

Figure 2: Estimated versus expected above-surface marine reflectance for model ζ^1 on 1%-noisy GLI data.

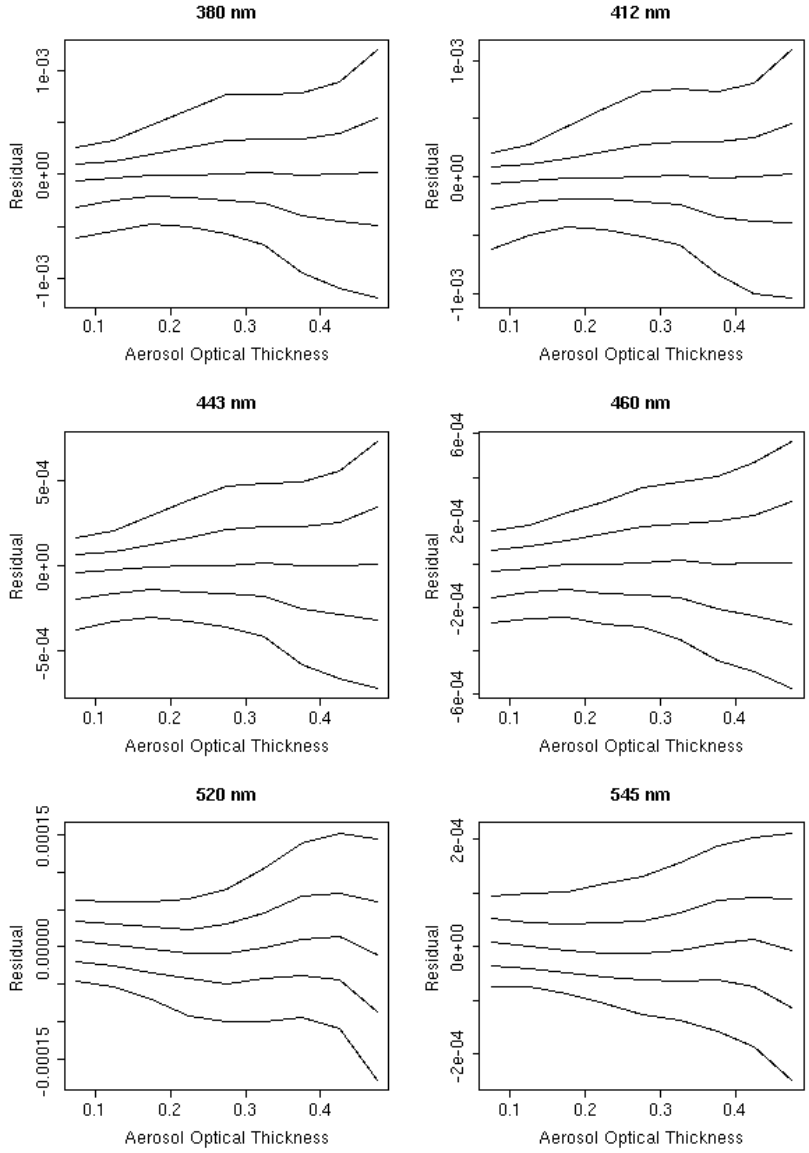

Figure 3: Conditional quantiles of order 5%, 25%, 50%, 75%, and 95% of the residual distributions as a function of aerosol optical thickness at 550 nm.

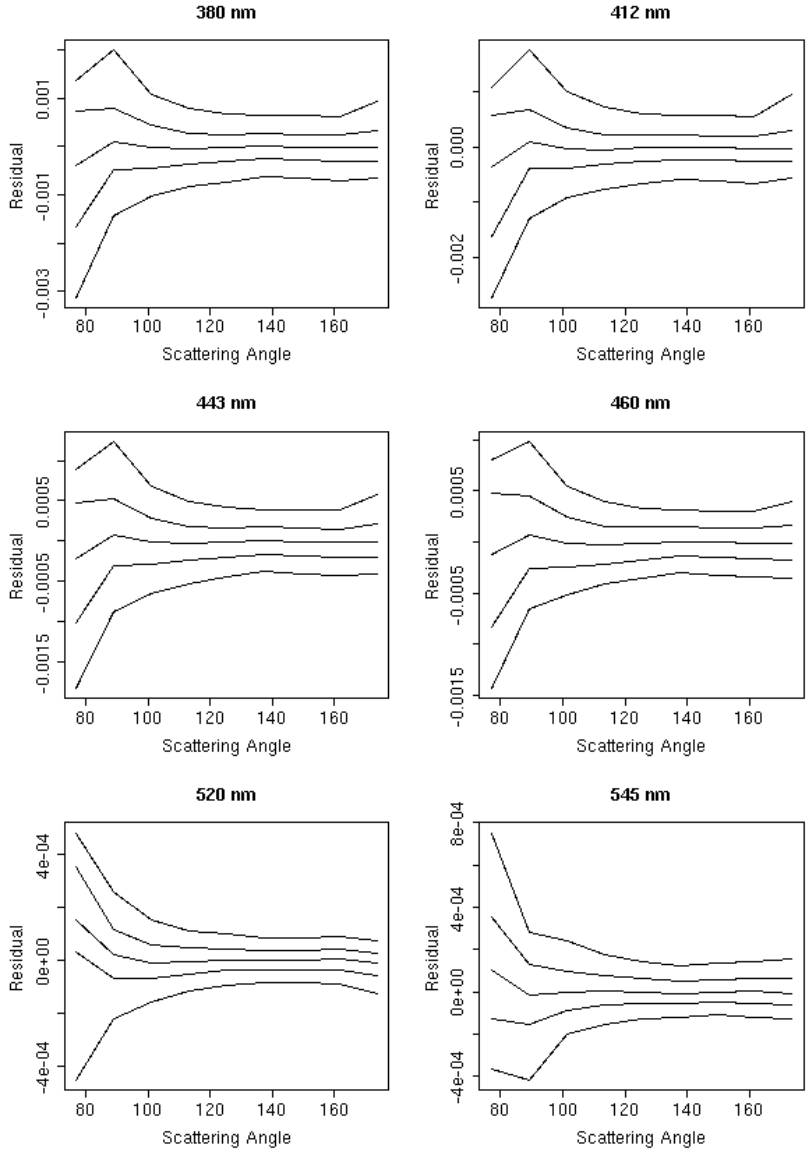

Figure 4: Conditional quantiles of order 5%, 25%, 50%, 75%, and 95% of the residual distributions as a function of scattering angle.

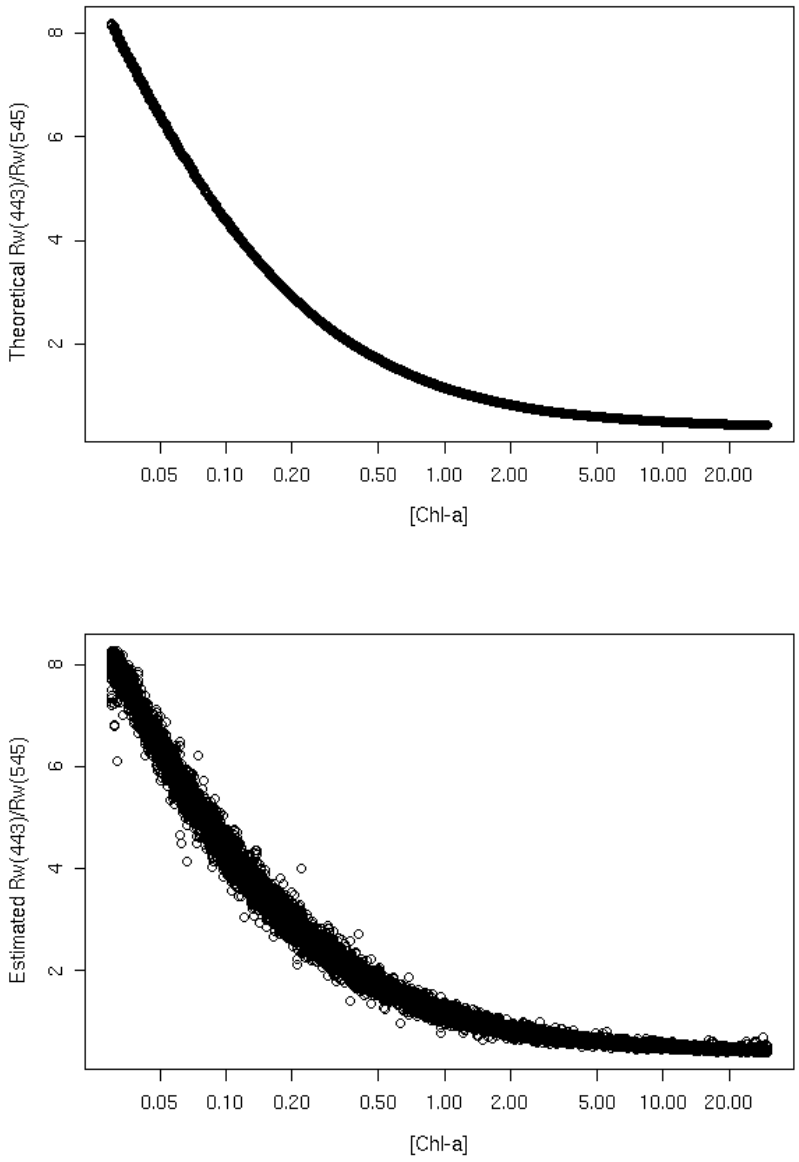

Figure 5: Ratio of marine reflectance at 443 and 545 nm as a function of chlorophyll-a concentration for theoretical reflectance (top) and for reflectance estimated by ζ^1 from 1%-noisy GLI data (bottom).

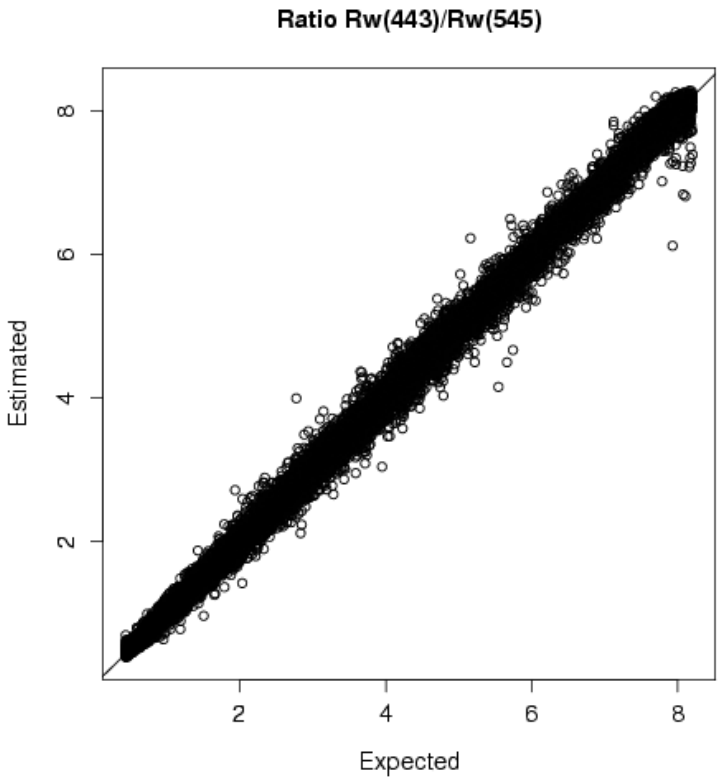

Figure 6: Estimated versus expected ratio of marine reflectance at 443 and 545 nm for model ζ^1 on 1%-noisy GLI data.